Lecture 28 Third order nonlinear optics

Origin of third order effects

The third (and other odd) order nonlinearities occur in all materials, whether they do have the center of inversion symmetry or not. We concentrate on materials that do have center of inversion. But there are two different ways in which the material may have a center of symmetry –it allows us to explain different 3rd order effects without quantum mechanics.

The first (most widely covered in textbooks) way of getting third order response is shown in Fig.28.1.a. Each polarizable entity, (atom, bond, or molecular orbital) has a center of inversion symmetry and is represented by a symmetric potential containing only the even orders of coordinates.

$$U(x) = -U_0 + \frac{Kx^2}{2} + \frac{Mx^4}{4} + ... \tag{28.1}$$

The second way, shown in Fig.28.1.b is different.) Each polarizable entity, (atom, bond, or molecular orbital) does not have a center of inversion symmetry, but for each "positive" entity there is also a "negative" entity-so the entire structure does have the center of inversion symmetry. While the individual dipoles at sum and differences frequencies are generated – the second order polarization terms are all zeroes. Due to cancelation of opposite sign terms. The potential can be written as

$$U(x) = -U_0 + \frac{Kx^2}{2} + \frac{L_{r(l)}x^3}{3} + ... \tag{28.2}$$

where Here r(l) is the right (left) entity and $L_r = -L_l$.

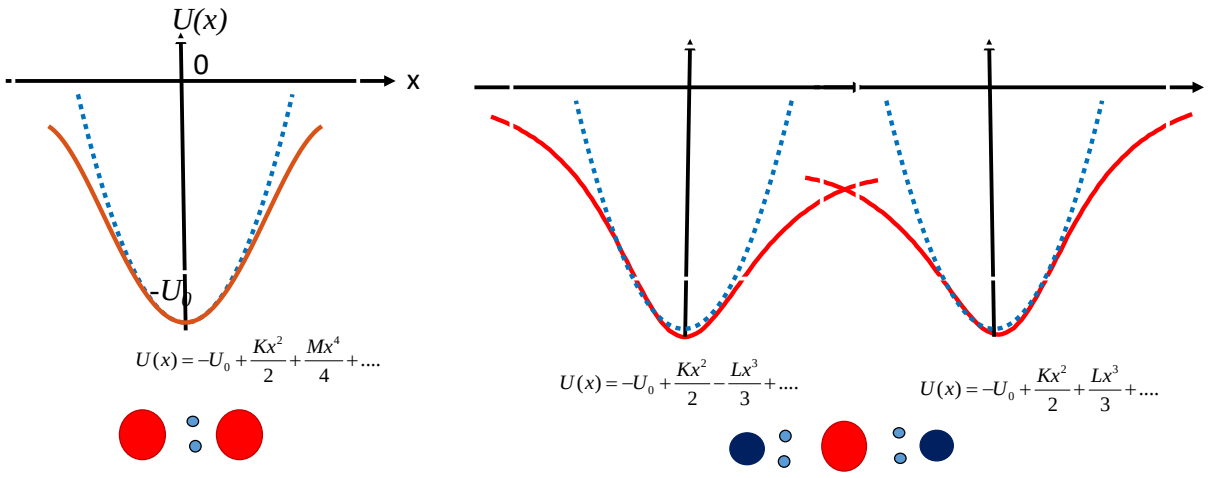

Figure 28.1 Origin of the third order nonlinear effects (a) Symmetric anharmonic oscillator (b)Two asymmetric anharmonic oscillators with the opposite signs of the odd order terms.

The equation of motion for the case of Fig.28.1.b is

$$m_0 \frac{d^2x}{dt^2} = -m_0\omega_0^2 x + L_{r(l)}x^2 - eE(t) \tag{28.3}$$

Let us assume the three-tone field,

$$E(t) = E_1 e^{-j\omega_1 t} + E_2 e^{-j\omega_2 t} + E_3 e^{-j\omega_3 t} + c.c. \tag{28.4}$$

Solution of (28.3) is expected to have linear, 2-nd-order, and third order terms,

$$\begin{aligned} x(t) &= \sum_{m=1}^{3} a_m E_m e^{-j\omega_m t} + \\ &+ \sum_{n=1}^{3}\sum_{m=1}^{3}\left(b_{mn}^{+} E_m E_n e^{-j(\omega_m+\omega_n)t} + b_{mn}^{-} E_m E_n^{*} e^{-j(\omega_m-\omega_n)t} \right) + \\ &+ \sum_{k=1}^{3}\sum_{n=1}^{3}\sum_{m=1}^{3}\left(c_{mnk}^{+} E_m E_n E_k e^{-j(\omega_m+\omega_n+\omega_k)t} + c_{mnk}^{-} E_m E_n^{*} E_k e^{-j(\omega_m-\omega_n+\omega_k)t} \right) + \ldots + c.c. \end{aligned} \tag{28.5}$$

Therefore we can find powers of $x(t)$ as

$$\begin{aligned} x^2(t) &= \left[\sum_{m=1}^{3} a_m E_m e^{-j\omega_1 t} + \sum_{n=1}^{3}\sum_{m=1}^{3}\left(b_{mn}^{+} E_m E_n e^{-j(\omega_m+\omega_n)t} + b_{mn}^{-} E_m E_n^{*} e^{-j(\omega_m-\omega_n)t} \right) \right]^2 = \\ &\sum_{n=1}^{3}\sum_{m=1}^{3}\left(a_m a_n E_m E_n e^{-j(\omega_m+\omega_n)t} + a_m a_n^{*} E_m E_n e^{-j(\omega_m-\omega_n)t} \right) + \ldots \\ &+ \sum_{k=1}^{3}\sum_{n=1}^{3}\sum_{m=1}^{3}\left(b_{mn}^{+} a_k E_m E_n E_k e^{-j(\omega_m+\omega_n+\omega_k)t} + (b_{mn}^{-} a_k + b_{mk}^{+} a_n^{*}) E_m E_n^{*} E_k e^{-j(\omega_m-\omega_n+\omega_k)t} \right) + \ldots + c.c. \end{aligned} \tag{28.6}$$

There are second order terms here, obtain by mixing two linear terms and the third order terms obtained by mixing the first and second order terms. The higher order terms are all neglected. Note the difference between the last two terms. Even though both of the oscillate at the same frequency $\omega_m - \omega_n + \omega_k$, in the first of them, $b_{mn}^{-} a_k$ the second order term oscillating at the difference frequency $\omega_m - \omega_n$ mixes with linear term at frequency $+\omega_k$. In the second case, $b_{mk}^{+} a_n^{*}$, the second order term oscillating at the difference frequency $\omega_m + \omega_k$ mixes with linear term at frequency $-\omega_n$. These terms therefore resonate at different frequencies as we shall see soon.

Third order susceptibility

Now, from the previous chapter we already know the first order response (27.9)

$$a_m = -\frac{e}{m_0(\omega_0^2 - \omega_m^2)} \tag{28.7}$$

and the second order response (27.13)

$$b_{mn}^{\pm} = \frac{2e^2 L_{r(l)}}{m_0^3(\omega_0^2-\omega_1^2)(\omega_0^2-\omega_2^2)\left[\omega_0^2-(\omega_1\pm\omega_2)^2\right]} \tag{28.8}$$

(It is easy to see that second order polarizations will cancel as $L_r = -L_l$). Now, substituting the third order terms from (28.5) and (28.6) into (28.3) we obtain

$$\begin{aligned} c_{mnk}^{+}\left[\omega_0^2-(\omega_m+\omega_n+\omega_k)^2\right]E_m E_n E_k e^{-j(\omega_m+\omega_n+\omega_k)t} &= \frac{6L_{r(l)}}{m_0} b_{mn}^{+} a_k E_m E_n E_k e^{-j(\omega_m+\omega_n+\omega_k)t} \\ c_{mnk}^{-}\left[\omega_0^2-(\omega_m-\omega_n+\omega_k)^2\right]E_m E_n^{*} E_k e^{-j(\omega_m+\omega_n+\omega_k)t} &= \frac{6L_{r(l)}}{m_0}(b_{mn}^{-} a_k + b_{mk}^{+} a_n^{*}) E_m E_n^{*} E_k e^{-j(\omega_m-\omega_n+\omega_k)t} \end{aligned} \tag{28.9}$$

The factor 6 comes from the fact the number of combinations by which the terms (m,n,k) can be obtained in a triple sum.

Therefore, in the response of the media we have 3-rd order polarization terms

$$P^{(3)}(\omega_4=\omega_1\pm\omega_2-\omega_3) = -Nec_{123}^{\pm}e^{-j(\omega_1\pm\omega_2+\omega_3)t} = 6\varepsilon_0\chi^{(3)}(\omega_4;\omega_1,\pm\omega_2,\omega_3)E_1 E_2^{(*)}E_3 e^{-j(\omega_1\pm\omega_2+\omega_3)t} + c.c. \tag{28.10}$$

Where we have introduced the third order susceptibility $\chi^{(3)}(\omega_4;\omega_1,\pm\omega_2,\omega_3)$ meaning that fields of three different frequencies mix and generate the fourth. Frequency. Third order susceptibility is a fourth rank tensor and one can in general write

$$\begin{aligned} \mathbf{P}^{(3)} &= \varepsilon_0\chi^{(3)}\mathbf{EEE} \\ P_i^{(3)} &= \varepsilon_0\sum_{j,k,l}\chi_{ijkl}^{(3)}E_j E_k E_l;\ i,j,k,l = x,y,z \end{aligned} \tag{28.11}$$

Consider now different ”flavors” of $\chi^{(3)}$, First of all, the one for the sum frequency generation

$$\chi^{(3)}(\omega_4;\omega_1,\omega_2,\omega_3) = \frac{Ne^4 L_{r(l)}^2}{\varepsilon_0 m_0^5(\omega_0^2-\omega_1^2)(\omega_0^2-\omega_2^2)\left[\omega_0^2-(\omega_1+\omega_2)^2\right](\omega_0^2-\omega_3^2)(\omega_0^2-\omega_4^2)} \tag{28.12}$$

Note that that in denominator you have four terms that provide resonance at each of four frequencies, i.e. $\omega_1,\omega_2,\omega_3$ and $\omega_4=\omega_1+\omega_2+\omega_3$,and, in addition the term resonating at sum frequency $\omega_1+\omega_2$.

For the sum/difference generation we have

$$\chi^{(3)}(\omega_4;\omega_1,\omega_2,-\omega_3)=\frac{Ne^4L_{r(l)}^2}{\varepsilon_0 m_0^5(\omega_0^2-\omega_1^2)(\omega_0^2-\omega_2^2)\left[\omega_0^2-(\omega_1+\omega_2)^2\right](\omega_0^2-\omega_3^2)(\omega_0^2-\omega_4^2)}$$
$$\chi^{(3)}(\omega_4;\omega_1,-\omega_2,\omega_3)=\frac{Ne^3L_{r(l)}^2}{\varepsilon_0 m_0^5(\omega_0^2-\omega_1^2)(\omega_0^2-\omega_2^2)\left[\omega_0^2-(\omega_1-\omega_2)^2\right](\omega_0^2-\omega_3^2)(\omega_0^2-\omega_4^2)} \quad (28.13)$$

The two "flavors" here are different. First resonates at sum frequency $\omega_1+\omega_2$, and the second at the beat frequency. $\omega_1-\omega_2$. The first "flavor" describes this sequence of events:

1. Field with frequency ω_1 causes oscillations of x at the same frequency
2. Field with frequency ω_2 via anharmonicity causes oscillations of x at the sum frequency $\omega_1+\omega_2$
3. Field with frequency ω_3 via anharmonicity causes oscillations of x at the sum frequency $\omega_1+\omega_2-\omega_3$

The second flavor describes a different sequence

1. Field with frequency ω_1 causes oscillations of x at the same frequency
2. Field with frequency ω_3 via anharmonicity causes oscillations of x at the beat frequency $\omega_1-\omega_3$
3. Field with frequency ω_2 via anharmonicity causes oscillations of x at the sum frequency $\omega_1+\omega_2-\omega_3$

Using the language of quantum mechanics we can say that for the first flavor a photon ω_1 is absorbed, then another photon ω_2 is absorbed, then photon ω_3 is emitted and we have polarization at $\omega_1+\omega_2-\omega_3$. For the second flavor the order is slightly changed ra photon ω_1 is absorbed, then another photon ω_3 is emitted, then photon ω_2 is absorbed and we have polarization at $\omega_1+\omega_2-\omega_3$. The change is small but the consequences will be important. Note since there is a term $L_{l(r)}^2$ in all the equations, the sign of $\chi^{(3)}$ below all resonances is positive.

If we now turn our attention to Fig.28.1.a, i.e. the case where each entity has center of inversion symmetry, the equation of motion is

$$m_0\frac{d^2x}{dt^2}=-m_0\omega_0^2x+Mx^3-eE(t) \quad (28.14)$$

where $E(t)$ is the same three-tone field (28.4). In the absence of even order terms, the response comprises only linear and third order terms

$$x(t)=\sum_{m=1}^{3}a_mE_me^{-j\omega_m t}+\sum_{k=1}^{3}\sum_{n=1}^{3}\sum_{m=1}^{3}\left(c_{mnk}^{+}E_mE_nE_ke^{-j(\omega_m+\omega_n+\omega_k)t}+c_{mnk}^{-}E_mE_n^{*}E_ke^{-j(\omega_m-\omega_n+\omega_k)t}\right)+...+c.c. \quad (28.15)$$

Taking a cube of a linear term, we obtain

$$x^3(t)=\left[\sum_{m=1}^{3}a_m E_m e^{-j\omega_m t}\right]^3=\sum_{k=1}^{3}\sum_{n=1}^{3}\sum_{m=1}^{3}\left(a_m a_n a_k E_m E_n E_k e^{-j(\omega_m+\omega_n+\omega_k)t}+a_m a_n a_k^* E_m E_n^* E_k e^{-j(\omega_m-\omega_n+\omega_k)t}\right)+c.c.$$

(28.16)

And upon substituting it into (28.14) we further obtain

$$\begin{aligned} c_{mnk}^{+}\left[\omega_0^2-(\omega_m+\omega_n+\omega_k)^2\right]E_m E_n E_k e^{-j(\omega_m+\omega_n+\omega_k)t}&=\frac{6M}{m_0}a_m a_n a_k E_m E_n E_k e^{-j(\omega_m+\omega_n+\omega_k)t}\\ c_{mnk}^{-}\left[\omega_0^2-(\omega_m-\omega_n+\omega_k)^2\right]E_m E_n^* E_k e^{-j(\omega_m+\omega_n+\omega_k)t}&=\frac{6M}{m_0}a_m a_n a_k^* E_m E_n^* E_k e^{-j(\omega_m-\omega_n+\omega_k)t}\end{aligned} \qquad (28.17)$$

The nonlinear polarization is

$$P^{(3)}(\omega_4=\omega_1\pm\omega_2-\omega_3)=-Nec_{123}^{\pm}e^{-j(\omega_1\pm\omega_2+\omega_3)t}=6\varepsilon_0\chi^{(3)}(\omega_4;\omega_1,\pm\omega_2,\omega_3)E_1 E_2^{(*)}E_3 e^{-j(\omega_1\pm\omega_2+\omega_3)t}+c.c.$$

(28.18)

And the third order susceptibility becomes

$$\chi^{(3)}(\omega_4;\omega_1,\pm\omega_2,\omega_3)=\frac{Ne^4M}{\varepsilon_0 m_0^4(\omega_0^2-\omega_1^2)(\omega_0^2\pm\omega_2^2)(\omega_0^2-\omega_3^2)(\omega_0^2-\omega_4^2)} \qquad (28.19)$$

There are resonances at each of three frequencies ω_{1-3} (single photon resonances) as well as three-photon resonance at frequency ω_4. However, two photon resonance $\omega_1+\omega_2$ at and beat frequency resonant $\omega_1-\omega_2$ are absent – but they represent the most important effects – two photon absorption, absorption saturation and nonlinear index.

It should be noted, that once one uses quantum mechanical description of nonlinear susceptibility, one will always have the resonances at $\omega_1+\omega_2$ and $\omega_1-\omega_2$ independent on whether local inversion symmetry is broken.

Order of magnitude.

In Chapter 27 we have established the relation between the size of the polarizable entity (atom, bond, molecule etc.) a_0 , the depth of the potential U_0 , (shown in Fig.28.2) and the coefficients K and L in (28.2) , namely

$$\begin{aligned} K&=m\omega_0^2\approx U_0/a_0^2\\ L&\approx U_0/a_0^3\end{aligned} \qquad (28.20)$$

It is easy to see that from the same considerations the scale of coefficient M in (28.1) is

$$M\approx U_0/a_0^4 \qquad (28.21)$$

Therefore, as long as one operates well below the resonance, we have and the expression for off-resonant third order susceptibility is (28.13) is

$$\chi_I^{(3)}(\omega_4;\omega_1,\omega_2,\omega_3)\approx\frac{Ne^4L_{r(l)}^2}{\varepsilon_0(m_0\omega_0^2)^5}\approx\frac{Ne^2}{\varepsilon_0 m_0\omega_0^2}\frac{\left(U_0/a_0^3\right)^2}{(U_0/a_0^2)^4}=\chi^{(1)}\left(\frac{a_0}{U_0/e}\right)^2\sim(n^2-1)F_a^{-2} \quad (28.22)$$

where according (27.35) the intrinsic (or atomic) field is

$$F_a=U_0/ea_0\sim10^{10}-10^{11}V/m \quad (28.23)$$

Therefore, since n²~2-15, $\chi^{(3)}\sim10^{-19}-10^{-22}m^2/V^2$.

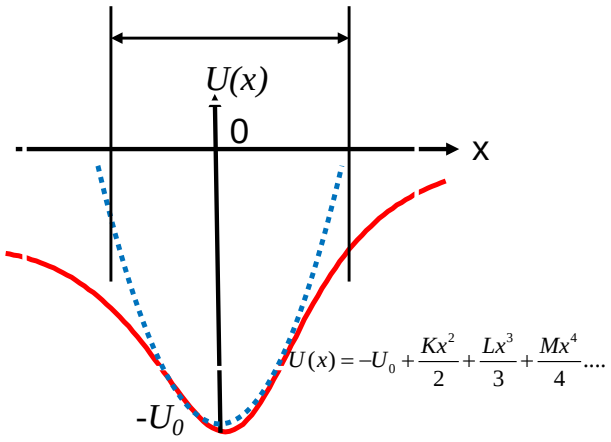

Figure 28.2 Finding the scale of third order susceptibility

If we substitute (28.21) into (28.19) we obtain

$$\chi_{II}^{(3)}(\omega_4;\omega_1,\pm\omega_2,\omega_3)\approx\frac{Ne^4M}{\varepsilon_0(m_0\omega_0^2)^4}\approx\frac{Ne^2}{\varepsilon_0 m_0\omega_0^2}\frac{U_0/a_0^4}{(U_0/a_0^2)^3}=(\varepsilon_r-1)\left(\frac{a_0}{U_0/e}\right)^2\sim\chi^{(1)}F_a^{-2} \quad (28.24)$$

i.e. essentially the same result as (28.22), Note a very strong dependence on resonance frequency – i.e. on the transparency band width. The materials that are transparent only in IR will have much larger nonlinearity, hence on should avoid comparing apples with oranges.

Sum frequency and 3rd harmonic generation

Consider the nonlinear polarization term at sum frequency,

$$\mathbf{P}^{(3)}(\omega_1+\omega_2+\omega_3)=6\varepsilon_0\chi^{(3)}(\omega_4;\omega_1,\omega_2,\omega_3)\mathbf{E}_{\omega_1}\mathbf{E}_{\omega_2}\mathbf{E}_{\omega_3} \quad (28.25)$$

and for simplicity, let us look at third harmonics $\omega_1=\omega_2=\omega_3=\omega$,

$$\mathbf{P}^{(3)}(3\omega)=\varepsilon_0\chi^{(3)}\mathbf{E}_\omega\mathbf{E}_\omega\mathbf{E}_\omega \quad (28.26)$$

Note that there is no factor of 6 for the degenerate case – because we do not have different combinations of 3 different fields. The situation is represented in Fig.28.4.a.

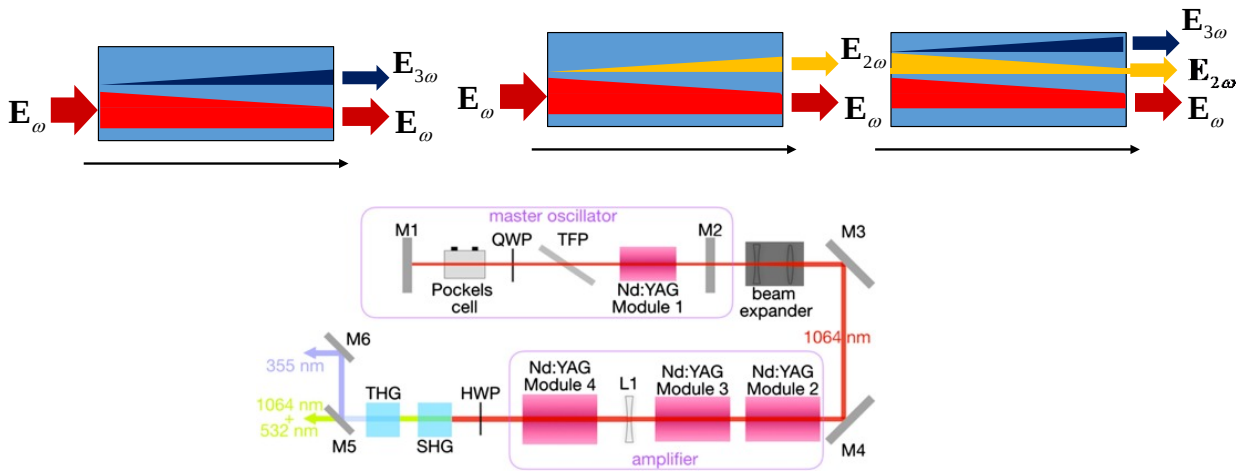

Figure 28.3 (a) Third harmonic generation using $\chi^{(3)}$ (b) Third harmonic generation using cascaded $\chi^{(2)}$ (c)Frequency doubling and tripling of Nd:YAG laser

Following previous chapter we introduce slow variable amplitudes for the fundamental and third harmonics, substitute nonlinear polarization (28.26) into the wave equation, and just like the case of SHG (Eq. 27.48) we obtain

$$\frac{dA_{3\omega}}{dz} = j\frac{3\omega}{2n_{3\omega}c}\chi^{(3)}_{eff}A^3_\omega e^{j\Delta kz} \tag{28.27}$$

where $\chi^{(3)}_{eff} = \hat{\mathbf{e}}_{3\omega}\cdot\chi^{(3)} : \hat{\mathbf{e}}_\omega \otimes \hat{\mathbf{e}}_\omega \otimes \hat{\mathbf{e}}_\omega$ and

$$\Delta k = 3k_\omega - k_{3\omega} = 3\frac{\omega}{c}(n_\omega - n_{3\omega}) \tag{28.28}$$

If we assume perfect phasematching undepleted fundamental pump,

$$\left|A_{3\omega}(L)\right|^2 = \left(\frac{3\pi L}{\lambda n_{3\omega}}\right)^2 \left|\chi^{(3)}_{eff}\right|^2 \left|A^3_\omega\right|^2 \tag{28.29}$$

The efficiency is quite small, much less than for the case of SHG. That is easy to see because for SHG we have the output power proportional to $\left|\chi^{(2)}_{eff}A^2_\omega\right|^2 \sim A^2_\omega\left(A_\omega / F_a\right)^2$ and for THG it is proportional to $\left|\chi^{(3)}_{eff}A^3_\omega\right|^2 \sim A^2_\omega\left(A^2_\omega / F^2_a\right)^2$. Since the optical field is always significantly less than "intrinsic" field F_a (otherwise the breakdown will ensue) it is easy that direct THG process sis far less efficient than SHG process.

For this reason one always uses "cascaded" generation – using second order nonlinearity as shown in Fig.28.3.b . First crystal produces SH and according to Eq. 27.52

$$\left|A_{2\omega}(L_1)\right|^2 = \left(\frac{2\pi L_1}{\lambda n_{2\omega}}\right)^2 \left|\chi^{(2)}_{eff,1}\right|^2 \left|A_\omega^2\right|^2 \tag{28.30}$$

In the second crystal SH is summed up with fundamental radiation to obtain 3rd harmonic $\omega + 2\omega = 3\omega$. The output amplitude squared is found as

$$\left|A_{3\omega}(L_2)\right|^2_{casc} = \left(\frac{6\pi L_2}{\lambda n_{3\omega}}\right)^2 \left|\chi^{(2)}_{eff,2}\right|^2 \left|A_\omega A_{2\omega}(L_1)\right|^2 = 9\left(\frac{2\pi\sqrt{L_1 L_2}}{\lambda\sqrt{n_{3\omega} n_{2\omega}}}\right)^4 \left|\sqrt{\chi^{(2)}_{eff,1}\chi^{(2)}_{eff,2}}\right|^4 \left|A_\omega^2\right|^3 \tag{28.31}$$

Now if we assume that $L_1 = L_2 = L; \chi^{(2)}_{eff,1,2} \sim \chi^{(2)}$ we can compare (28.31) with the direct THG generation result (28.29)

$$\frac{\left|A_{3\omega}(L)\right|^2_{casc}}{\left|A_{3\omega}(L)\right|^2_{dir}} = \left(\frac{4\pi L}{\lambda n_{2\omega}}\right)^2 \frac{\left|\chi^{(2)}\right|^4}{\left|\chi^{(3)}\right|^2} \tag{28.32}$$

Now using (28.22) we obtain

$$\frac{\left|\chi^{(2)}\right|^2}{\left|\chi^{(3)}\right|} \approx \frac{\left(\chi^{(1)} F_a^{-1}\right)^2}{\chi^{(1)} F_a^{-2}} = \chi^{(1)} \approx n^2 \tag{28.33}$$

Therefore

$$\frac{\left|A_{3\omega}(L_2)\right|^2_{casc}}{\left|A_{3\omega}(L_2)\right|^2_{dir}} \sim \left(\frac{4\pi nL}{\lambda}\right)^2 >> 1 \tag{28.34}$$

Cascaded (sequential) process is always far more efficient than direct process. That is why third harmonic is always obtained this way as is indeed shown in Fig.28.3.c where frequency doubling and tripling of a powerful Nd:YAG laser/amplifier is shown.

Two-photon absorption (TPA)

In case of second harmonic generation the phase of nonlinear susceptibility usually does not matter – having imaginary part of second order polarization only means relative phase shift. This is not always the case for the third order susceptibility where imaginary part of nonlinear polarization may mean chane of amplitude, i.e. absorption, or gain. Consider the nonlinear susceptibility term that shows two-photon resonance, at sum frequency (28.13). Because we operate clos eto resonance we must include damping term γ

$$\chi^{(3)}(\omega_4;\omega_1,\omega_2,-\omega_3)=\frac{Ne^4L_{r(l)}^2}{\varepsilon_0 m_0^5(\omega_0^2-\omega_1^2)(\omega_0^2-\omega_2^2)\left[\omega_0^2-(\omega_1+\omega_2)^2-j(\omega_1+\omega_2)\gamma\right](\omega_0^2-\omega_3^2)(\omega_0^2-\omega_4^2)} \tag{28.35}$$

We consider the case when $\omega_2=\omega_3$ and then $\omega_4=\omega$. We also assume that we operate close to the two photon resonance, $\omega_1+\omega_2\approx\omega_0$, then

$$\chi^{(3)}(\omega_1;\omega_1,\omega_2,-\omega_2)\approx\frac{Ne^4L_{r(l)}^2}{\varepsilon_0 m_0^5\omega_0^8\left[\omega_0^2-(\omega_1+\omega_2)^2-j(\omega_1+\omega_2)\gamma\right]}\approx\chi_{nonres}^{(3)}\frac{\omega_0/2}{\omega_0-(\omega_1+\omega_2)-j\gamma/2} \tag{28.36}$$

where $\chi_{nonres}^{(3)}$ is non-resonant susceptibility estimated in (28.22). As one can see the resonant nonlinearity can exceed nonresonant one by $Q=\omega_0/\gamma$. The dispersion of $\chi^{(2)}$ in the vicinity of resonance is Lorentzian. Consider the imaginary part of (28.36)

$$\chi_{im}^{(3)}(\omega_1;\omega_1,\omega_2,-\omega_2)\approx\chi_{nonres}^{(3)}\frac{\omega_0\gamma/4}{\left[\omega_0-(\omega_1+\omega_2)\right]^2+\gamma^2/4} \tag{28.37}$$

The \imaginary part of nonlinear polarization is

$$P^{(3)}(\omega_1)\approx j\varepsilon_0 2\chi_{nonres}^{(3)}\frac{\omega_0\gamma/4}{\left[\omega_0-(\omega_1+\omega_2)\right]^2+\gamma^2/4}A_1\left|A_2\right|^2e^{jk_1z-j\omega_1t}\approx j\varepsilon_0 2\chi_{nonres}^{(3)}QA_1\left|A_2\right|^2e^{jk_1z-j\omega_1t} \tag{28.38}$$

Note that the phase matching is always preserved $k_4=k_1+k_2-k_2=k_1$. Now, substitute (28.38) into the slowly variable amplitude equation and obtain

$$\frac{dA_1}{dz}=j\frac{\omega_1}{2n_1c\varepsilon_0}P^{(3)}(\omega_1)=-\frac{\pi}{n\lambda_1}2\chi_{nonres}^{(3)}Q\left|A_2\right|^2A_1 \tag{28.39}$$

Introducing power densities

$$S_{1,2}=2n_{1,2}\,|\,A_{1,2}\,|^2/\eta_0 \tag{28.40}$$

we transform (28.39) into

$$\frac{dS_1}{dz}=-\frac{\pi}{2n_1n_2\lambda_1}\chi_{nonres}^{(3)}Q\eta_0S_2S_1=-2\beta S_2S_1 \tag{28.41}$$

where we have introduced TPA coefficient

$$\beta=\frac{\pi}{4n\lambda_1}\chi_{nonres}^{(3)}Q\eta_0\ \ (cm/W) \tag{28.42}$$

Consider now the degenerate case $\omega_1 = \omega_2 = \omega$. Equation (28.41) becomes

$$\frac{dS}{dz} = -\beta S^2 \tag{28.43}$$

(note that factor 2 is absent for the degenerate case. Solution is

$$S(z) = \frac{S(0)}{1 + S(0)\beta z} \tag{28.44}$$

and it is plotted in Fig.28.4 in the same plot with the linear absorption (both on arbitrary scales) As one can see TPA decreases as the intensity of light decreases.

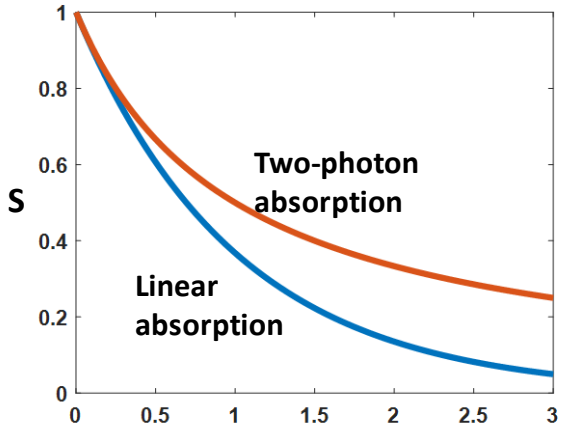

Figure 28.4 Decrease of optical power vs propagation length for the linear absorption and TPA .

The two-photon nature of the process can be understood if one notes that $\chi^{(3)}(\omega_1;\omega_1,\omega_2,-\omega_2) = \chi^{(3)}(\omega_2;\omega_2,\omega_1,-\omega_1)$ and equation (28.41) works for powers at frequencies ω_1 and ω_2 ,i.e.

$$\begin{aligned} \frac{dS_1}{dz} &= -\frac{\pi}{2n_1 n_2 \lambda_1}\chi^{(3)}_{nonres} Q\eta_0 S_2 S_1 \\ \frac{dS_2}{dz} &= -\frac{\pi}{2n_1 n_2 \lambda_2}\chi^{(3)}_{nonres} Q\eta_0 S_2 S_1 \end{aligned} \tag{28.45}$$

But photon flux densities are

$$N_{1,2} = \frac{S_{1,2}}{\hbar\omega_{1,2}} = \frac{2\pi\lambda_{1,2}}{\hbar c} S_{1,2} \tag{28.46}$$

and

$$\frac{dN_1}{dz} = -\frac{\pi\hbar c\eta_0}{4n_1n_2\lambda_1\lambda_2}\chi^{(3)}_{nonres}QN_2N_1 = -\kappa N_2N_1$$
$$\frac{dN_2}{dz} = -\frac{\pi\hbar c\eta_0}{4n_1n_2\lambda_2\lambda_1}\chi^{(3)}_{nonres}Q\eta_0N_1N_2 = -\kappa N_2N_1 \qquad (28.47)$$

The meaning of (28.47) is that Two photons must be absorbed simultaneously to conserve energy as the atom (molecule) absorbs the energy of photons.

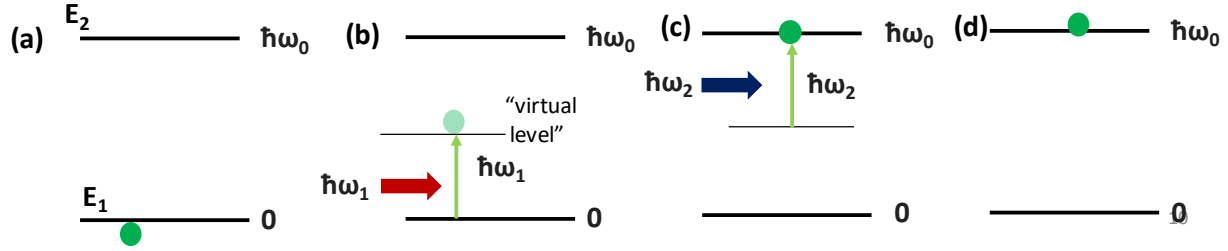

Figure 28.5. Quantum description of TPA.

Let us now consider Quantum description of TPA as schematically represented in Fig.28.5. (a-d). The medium is represented here as a two level system with two levels separated by energy $\mathrm{E}_2 - \mathrm{E}_1 = \hbar\omega_0$. Originally (a) the electron is in the lower energy state. Then photon of frequency ω_1 arrives and gets absorbed (b). The energy is obviously not conserved, and one says that the electron is at the "virtual energy level". According to the uncertainty principle the electron can stay there for the time $\Delta\tau \approx 1/\Delta\mathrm{E}=1/\hbar(\omega_0-\omega_1)$. So a second photon with frequency ω_2 must arrive within this very short (typically less than a femtosecond) interval as shown in (c) – at this point the energy conservation is restored and the electron can safely rest on the level 2 (d)

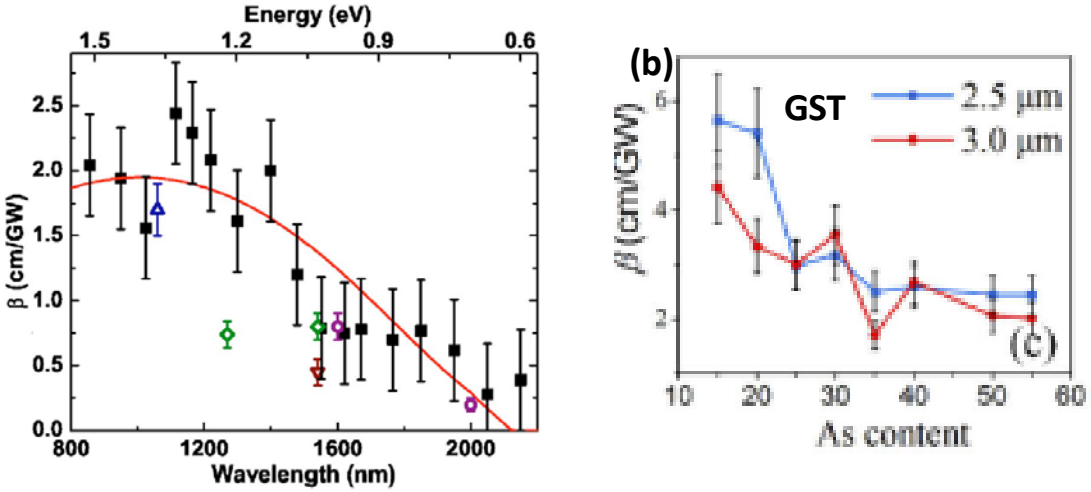

Figure 28.6 TPA in (a) Si (b)Ge-As-Te glass

The order of magnitude for TPA coefficient given by the Eq. (28.42) can be found by noting for wavelength of $\lambda \sim 1\mu m$ by noting that for solid state with broad absorption band maximum $Q_{\max} \sim 10$ and also that $\chi^{(3)}_{nres} \sim 10^{-19} - 10^{-21} m^2 / V^2$. With that $\beta \sim 10^{-10} - 10^{-8} cm / W$. In Fig.28.6.a spectrum of TPA coefficient β in Si is shown. Note that β appears only at wavelength shorter than twice wavelength of the absorption edge of Si i.e. at 2000nm. For the integrated optics one operate sin the region 1300-1500nm –and TPA there is high. Therefore, in the so-called "silicon photonics" waveguides are often made from silicon nitride Si_3N_4 which has higher bandgap and no TPA absorption in the 1300-1500nm range. Sometimes TPA can be useful rather than deleterious and one can find materials with higher β, such as Ge-As-Te chalcogenide glass (GST) as shown in Fig.28.6.b as a function of As content.

Optical limiting

Consider now application of TPA in optical limiting. The ide of optical limiter is to protect a sensitive detector, or an eye from powerful laser radiation which tries to blind the detector or a person. There are different types of optical limiters – reflective, self-de-focusing, and, relevant to TPA, absorptive. As shown in Fig.28.7.a absorptive limiter has low transmission for weak signal and high transmission for strong signal. The ideal characteristic of limiter is shown in Fig.28.7b , as long as input power density is less than $S_{\max}$ 100% of input power is transmitted and $S_{out} = S_{in}$, but when input power density exceeds $S_{\max}$, the output power density gets clamped at $S_{out} = S_{\max}$. The non-idea optical limiter operates according to (28.44)

$$S_{out} = \frac{S_{in}}{1 + S_{in}\beta L} = \frac{S_{in}}{1 + S_{in} / S_{sat}} \tag{28.48}$$

where saturation power density is $S_{sat} = 1/\beta L \sim 0.1 GW / cm^2$. As one can see from Fig.28.7c the output power does saturate at $S_{out} = S_{sat}$ when $S_{in} >> S_{sat}$

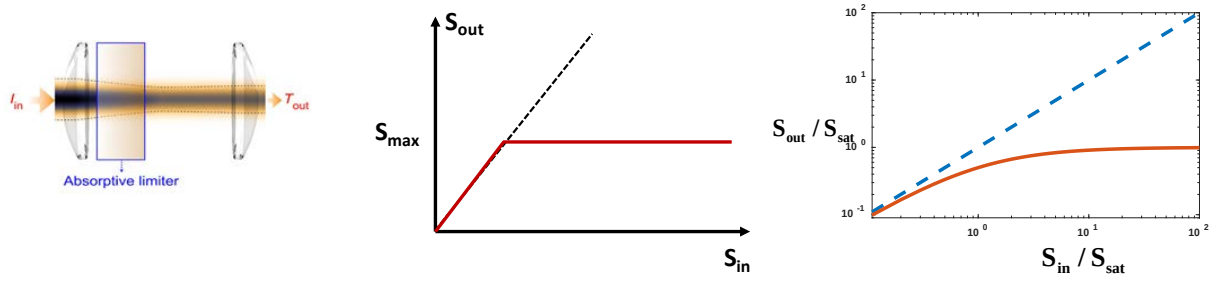

Figure 28.7 (a) optical limiter based on TPA (b) transmission characteristics of an ideal limiter (c) transmission characteristics of a typical limiter.

Nonlinear phase shift

Consider now the real part of the resonant nonlinear susceptibility (28.36)

$$\chi^{(3)}_{r,TPA}(\omega_1;\omega_1,\omega_2,-\omega_2)=\frac{Ne^4L^2_{r(l)}}{\varepsilon_0 m_0^5(\omega_0^2-\omega_1^2)^2(\omega_0^2-\omega_2^2)^2\left[\omega_0^2-(\omega_1+\omega_2)^2-j(\omega_1+\omega_2)\gamma\right]}\sim$$

$$\sim\chi^{(3)}_{nonres}\frac{\omega_0\left[\omega_0-(\omega_1+\omega_2)\right]}{\left[\omega_0-(\omega_1+\omega_2)\right]^2+\gamma^2/4} \qquad (28.49)$$

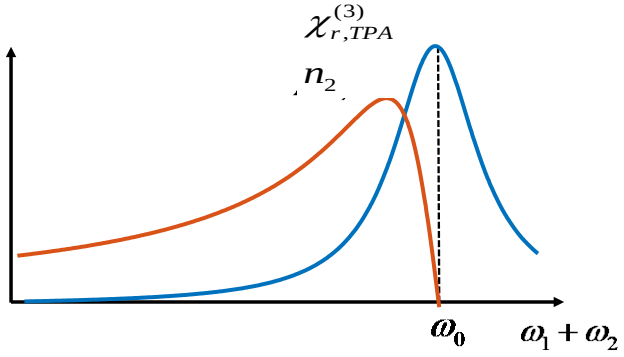

Figure 28.8 Dispersion of TPA and third order nonlinear susceptibility with nonlinear index

The off-resonant TPA – is just a Lorentzian that peaks in the vicinity of TPA resonance, as shown in Fig. 28.8 This term is a nonlinear phase delay, hence it describes nonlinear index. Let us find the nonlinear polarization as

$$P^{(3)}_{r,TPA}(\omega_1)=\varepsilon_0\chi^{(3)}_{r,TPA}(\omega_1;\omega_1,\omega_2,-\omega_2)A_1A_2A_2^*e^{j(k_1z-\omega_1t)}+\varepsilon_0\chi^{(3)}_{r,TPA}(\omega_1;\omega_2,\omega_1,-\omega_2)A_2A_1A_2^*e^{j(k_1z-\omega_1t)}\approx$$

$$\approx 2\varepsilon_0\chi^{(3)}_{r,TPA}A_1\left|A_2\right|^2e^{j(k_1z-\omega_1t)}$$

(28.50)

Factor of two appears because the order of ω_1 and ω_2 (i.e. which photon comes first) can be changed. We substitute it into the wave equation for wave ω_1 and get

$$\nabla^2A_1+\frac{\omega_1^2n_{1,0}^2}{c^2}A_1=-\frac{\omega_1^2}{c^2}2\chi^{(3)}_{r,TPA}A_1\left|A_2\right|^2 \qquad (28.51)$$

where $n_{1,0}$ is the refractive index at frequency ω_1 in the absence of nonlinear interaction. Re-write (28.51) as

$$\nabla^2A_1+\frac{\omega_1^2}{c^2}\left(n_{1,0}^2+2\chi^{(3)}_{r,TPA}\left|A_2\right|^2\right)A_1=0 \qquad (28.52)$$

Clearly, the expression in the parenthesis is a new dielectric constant,

$$n_1^2=n_{1,0}^2+2\chi^{(3)}_{r,TPA}\left|A_2\right|^2=n_{1,0}^2+\chi^{(3)}_{r,TPA}\eta_0S_2/n_{2,0} \qquad (28.53)$$

Where we have introduced power density $S_2=2n_2\,|\,A_2\,|^2/\eta_0$ from (28.40). The new refractive index can then be found as

$$n_1 = \sqrt{n_1^2} \approx n_{1,0} + \chi^{(3)}_{r,TPA}\eta_0 S_2 / 2n_{1,0}n_{2,0} = n_{1,0} + 2\mathrm{n}_2 S_2 \tag{28.54}$$

where we have introduced the nonlinear refractive index (note the roman, non-italicized font)

$$\mathrm{n}_2 = \chi^{(3)}_{r,TPA}\eta_0 / 4n_{1,0}n_{2,0} \approx \chi^{(3)}_{r,TPA}\eta_0 / 4n^2 \tag{28.55}$$

Order of magnitude of n_2 is $\mathrm{n}_2 \sim 10^{-17} - 10^{-20} m^2 / W$.

If we consider degenerate case, then

$$P^{(3)}_{r,TPA}(\omega_1) = \varepsilon_0 \chi^{(3)}_{r,TPA}(\omega_1; \omega_1, \omega_1, -\omega_1) A_1 A_2 A_2^* e^{-j\omega_1 t} \approx \varepsilon_0 \chi^{(3)}_{r,TPA} A_1 \left|A_1\right|^2 e^{-j\omega_1 t} \tag{28.56}$$

Therefore, for two fields interacting one has both self-modulation and cross-modulation terms

$$\begin{aligned} n_1 &= n_{1,0} + \mathrm{n}_2 S_1 + 2\mathrm{n}_2 S_2 \\ n_2 &= n_{2,0} + \mathrm{n}_2 S_2 + 2\mathrm{n}_2 S_1 \end{aligned} \tag{28.57}$$

Quantum description of nonlinear phase modulation

We consider the same two-level description of nonlinear medium as when we looked at TPA in Fig.28.5.

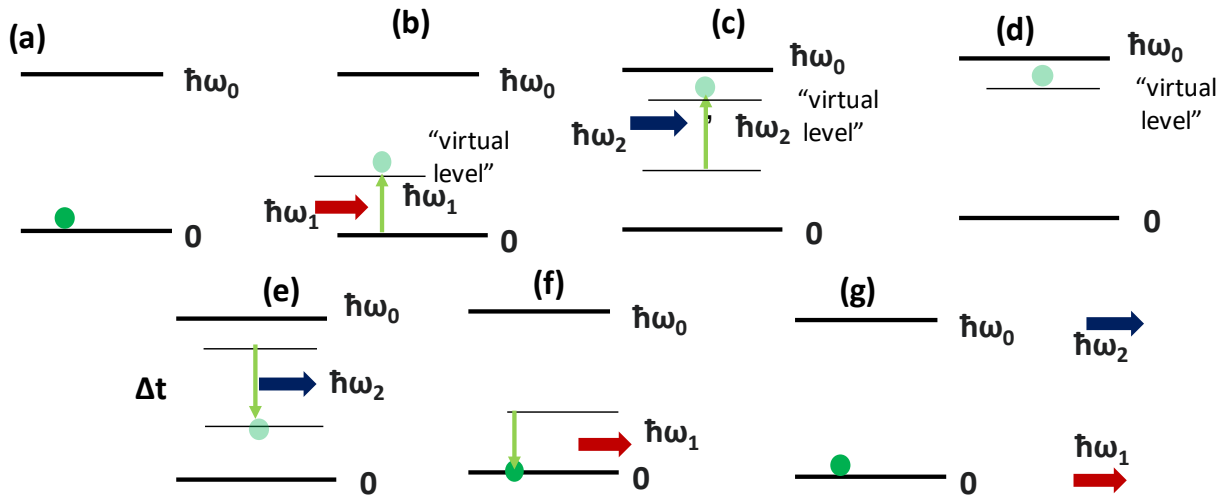

Figure 28.9 Quantum mechanical interpretation of nonlinear refractive index

A shown in Fig.28.9a and b the electron makes a transition to the virtual level when photon ω_1 arrives and gets absorbed. When the second photon arrives shortly thereafter (Fifg.28.8.c) the electron makes transition to another virtual level, detuned from the upper level because the energy of two photons is not sufficient for the electron to make a transition to the real level. The electron spends time $\Delta t \sim 1/\hbar(\omega_0 - \omega_1 - \omega_2)$ in this second virtual level, as required by the uncertainty principle (Fig.28.9.d). One can say that the energy of two photons has been transferred into the energy of "spring" oscillations. Then the energy is released, first to the photon with frequency ω_2 (Fig.28.9.e) and then nearly instantaneously to the second photon with frequency ω_1 (Fig.28.9.e). (Of course, the order can be

changed). Finally the electron is back in the ground state (Fig.28.9.g) and the two photons are still propagating, but due to delay Δt their phases have changed. One can see that phase delay at one frequency depends on the intensity of the other frequency.

Nonlinearity due to absorption saturation

In addition to resonant nonlinearity that occurs due to two-photon resonance (28.49), nonlinearity also gets enhanced when one photon-resonance is present, i.e. $\omega_{1(2)} \to \omega_0$.

$$\chi^{(3)}_{r,sat}(\omega_1;\omega_1,-\omega_2,\omega_2) \sim \chi^{(3)}_{nonres} \frac{\omega_0^4}{\left[(\omega_0-\omega_1)^2+\gamma^2/4\right]\left[(\omega_0-\omega_2)^2+\gamma^2/4\right]} \tag{28.58}$$

This term peaks near the linear absorption peak and is usually related to absorption. It usually has negative sign. It can be construed as the result of saturation. In quantum theory, when the atom (or bond) absorbs a photon it is no longer active. As the number of active atoms gets reduced, so does the susceptibility. The situation is shown in Fig. 28.10. On the absence of radiation all atoms are in the lower state (a), but when the radiation with power density S is present some of them get excited to the upper state (b).

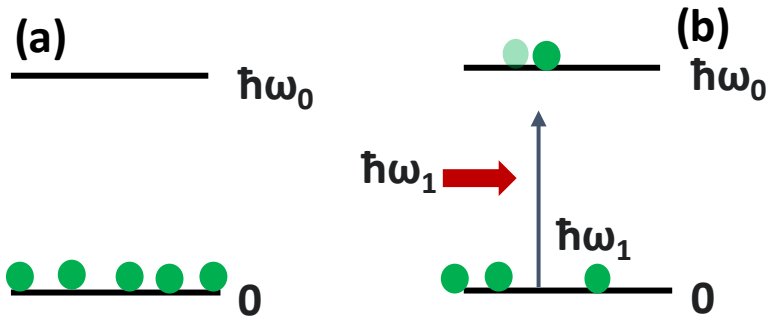

Figure 28.10 Nonlinearity due to absorption saturation

Near resonance we can write for the density of active atoms at lower level

$$\frac{dN_a}{dt} = -\alpha\frac{S}{\hbar\omega} + \frac{N_{a0}-N_a}{\tau} \tag{28.59}$$

where α is absorption coefficient, τ is characteristic relaxation time and N_{a0} is the active atom density in the absence of light. Introduce $\Delta N_a = N_{a0} - N_a$, then we can write (28.59) as

$$\frac{d\Delta N_a}{dt} = \alpha\frac{S}{\hbar\omega} - \frac{\Delta N_a}{\tau} \tag{28.60}$$

Consider two-tone input of two waves with frequencies $\omega_{1,2}$. The time-averaged over a few optical periods power density is

$$S(t)=\left\langle E(t)^2\right\rangle n/\eta_0=\frac{n}{\eta_0}\left\langle (A_1e^{-j\omega_1 t}+A_2e^{-j\omega_2 t}+c.c)(A_1e^{-j\omega_1 t}+A_2e^{-j\omega_2 t}+c.c)\right\rangle=$$

$$=\frac{n}{\eta_0}\left\langle 2A_1A_1^*+2A_2A_2^*+2A_1A_2^*e^{-j(\omega_1-\omega_2)t}+2A_1^*A_2e^{+j(\omega_1-\omega_2)t}+2A_1^2e^{-2j\omega_1 t}+2A_2^2e^{-2j\omega_2 t}+2A_1A_2e^{-j(\omega_1+\omega_2)t}+2A_2^*A_2^*e^{+j(\omega_1+\omega_2)t}\right\rangle$$

(28.61)

As long as $\Delta\omega=\omega_1-\omega_2$ is small (more precisely $1/\Delta\omega$ is longer than detector response)

$$S(t)=\frac{n}{\eta_0}\left[2\left|A_1\right|^2+2\left|A_2\right|^2+2(A_1^*A_2e^{+j(\omega_1-\omega_2)t}+c.c.)\right]=S_1+S_2+2\sqrt{S_1S_2}\cos\left[(\omega_1-\omega_2)t\right]$$

(28.62)

where $S_{1,2}$ are the individual power densities and the last term oscillates at beat frequency $\Delta\omega$. Let us look for a solution of (28.60) as

$$\Delta N_a=N_1+N_+e^{-j\Delta\omega t}+N_-e^{j\Delta\omega t} \tag{28.63}$$

Substitution yields

$$-jN_+e^{-j\Delta\omega t}+jN_-e^{j\Delta\omega t}=\alpha\frac{S_1+S_2+\sqrt{S_1S_2}e^{-j\Delta\omega t}+\sqrt{S_1S_2}e^{-j\Delta\omega t}}{\hbar\omega}-\frac{N_1+N_+e^{-j\Delta\omega t}+N_-e^{j\Delta\omega t}}{\tau}$$

(28.64)

And combining the terms with the same temporal dependencies, we arrive at

$$\begin{aligned}N_1&=\frac{\alpha\tau}{\hbar\omega}\left(S_1+S_2\right);\\ N_\pm&=\frac{\alpha\tau}{\hbar\omega}\sqrt{S_1S_2}\,\frac{\tau}{1\mp j\Delta\omega\tau}e^{\mp j\Delta\omega t}\end{aligned} \tag{28.65}$$

Change of the number of active atoms will cause the change of linear susceptibility

$$\chi(\omega_{1,2})=\frac{N_ae^2}{\varepsilon_0m_0(\omega_0^2-\omega^2)}=\frac{\left(N_a-\Delta N_a\right)e^2}{\varepsilon_0m_0(\omega_0^2-\omega_{1,2}^2)}=\chi_0(\omega_{1,2})-\Delta\chi(\omega_{1,2}) \tag{28.66}$$

Hence

$$\Delta\chi(\omega_{1,2})=\chi(\omega_{1,2})\frac{\Delta N_a}{N_a}=\frac{\chi(\omega_{1,2})\tau}{N_a\hbar}\left[\frac{\alpha_1}{\omega_1}S_1+\frac{\alpha_2}{\omega_2}S_2+\frac{1}{1-j\Delta\omega\tau}\sqrt{\frac{\alpha_1\alpha_2}{\omega_1\omega_2}S_1S_2}e^{-j\Delta\omega t}+\frac{1}{1+j\Delta\omega\tau}\sqrt{\frac{\alpha_1\alpha_2}{\omega_1\omega_2}S_1S_2}e^{j\Delta\omega t}\right]\approx$$

$$\approx\frac{\chi(\omega_{1,2})\alpha\tau}{N_a\hbar\omega}\left[S_1+S_2+\frac{1}{1-j\Delta\omega\tau}\sqrt{S_1S_2}e^{-j\Delta\omega t}+\frac{1}{1+j\Delta\omega\tau}\sqrt{S_1S_2}e^{j\Delta\omega t}\right]$$

(28.67)

Then third order nonlinear polarization can be found at each frequency as simply

$$P_{sat}^{(3)}(\omega_1) = -\frac{\varepsilon_0 \chi(\omega_1)\alpha\tau}{N_a \hbar\omega}\left[S_1 A_1 e^{-j\omega_1 t} + S_2 A_1 e^{-j\omega_1 t} + \frac{1}{1 - j\Delta\omega\tau}\sqrt{S_1 S_2}\, e^{j\Delta\omega t} A_2 e^{-j\omega_2 t}\right] =$$
$$= -\frac{2\varepsilon_0 \chi(\omega_1)\alpha n\tau}{N_a \hbar\omega\eta_0}\left[A_1 A_1^* A_1 e^{-j\omega_1 t} + A_2 A_2^* A_1 e^{-j\omega_1 t} + \frac{A_1 A_2^*}{1 - j\Delta\omega\tau} A_2 e^{-j\omega_1 t}\right] \tag{28.68}$$

One can see that the first term is self-saturation, the second term is cross-saturation and the third term is more interesting – it occurs due to modulation of active atom density at beat frequency which in terms modulates the incoming wave A_2 so a side-band at frequency ω_1 is generated. In quantum description the oscillations of active atom density is called coherent population oscillations. Thus we have two components to the susceptibility

$$\chi_{sat}^{(3)}(\omega_1;\omega_2,-\omega_2,\omega_1) \sim -\frac{2\chi(\omega)\alpha n\tau}{N_a \hbar\omega\eta_0}$$
$$\chi_{beat}^{(3)}(\omega_1;\omega_1,-\omega_2,\omega_2) \sim -\frac{2\chi(\omega)\alpha n\tau}{N_a \hbar\omega\eta_0}\frac{1}{1 - j\Delta\omega\gamma} \tag{28.69}$$

Since linear susceptibility in general has both imaginary and real parts, $\chi(\omega) = \chi'(\omega) + j\chi''(\omega)$ so does the third order susceptibility $\chi^{(3)} = \chi^{(3)'} + j\chi^{(3)''}$ – in other words we have two nonlinear effects – saturation of absorption and nonlinear refractive index

$$\mathrm{n}_{2,sat} \sim -\frac{\chi'(\omega)\alpha\tau}{N_a \hbar\omega}$$
$$\mathrm{n}_{2,beat} \sim -\frac{\chi'(\omega)\alpha\tau}{N_a \hbar\omega}\frac{1}{\sqrt{1 + (\Delta\omega\tau)^2}} \tag{28.70}$$

Since $\alpha(\omega) = \frac{\omega}{nc}\chi''(\omega)$, we finally obtain

$$\mathrm{n}_{2,sat} \sim -\frac{\chi'(\omega)\chi''(\omega)\tau}{N_a \hbar c}$$
$$\mathrm{n}_{2,beat} \sim -\frac{\chi'(\omega)\chi''(\omega)\tau}{N_a \hbar c}\frac{1}{\sqrt{1 + (\Delta\omega\tau)^2}} \tag{28.71}$$

Dispersion of this nonlinear index is quite resonant since both real and especially imaginary part of linear susceptibility are resonant. This can be seen in Fig. 28.11 (a) where we plot nonlinear absorption

$$\beta_{sat} = \frac{\omega}{nc}\chi_{sat}^{(3)''} = -\frac{\omega\tau}{N_a \hbar c^2}\left|\chi''(\omega)\right|^2 \quad (m/W) \tag{28.72}$$

and n_2. Also shown in Fig, 28.11.b is the TPA and nonlinear index due to it (same as Fig.28.8). Adding two effects results in the spectra of combined nonlinear absorption and nonlinear index in Fig.28.11c. One can see the sign change occurring somewhere beyond ½ of transmission range. Normally we operate below 0.5 ω_0 – below half-bandgap to avoid TPA.

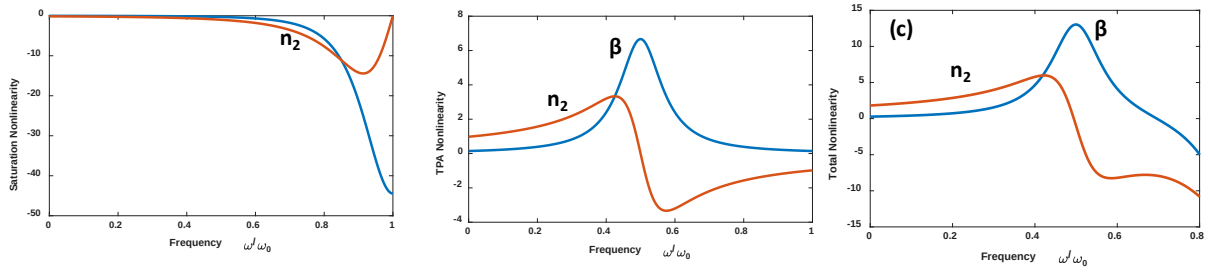

Figure 28.11. Nonlinear index and nonlinear absorption spectral dependencies (a) due to saturation (b) due to TPA (c) combined.

If we now look at experimental data on dispersion of nonlinear index in three different materials: Si, GaN and C (diamond) in Fig.28.12 a-c, we can see that the curves broadly follow those of Fig.28.11.c – positive at low frequencies, then increasing to the peak value slightly above half of bandgap energy, then decreasing and changing sign to negative near the absorption edge.

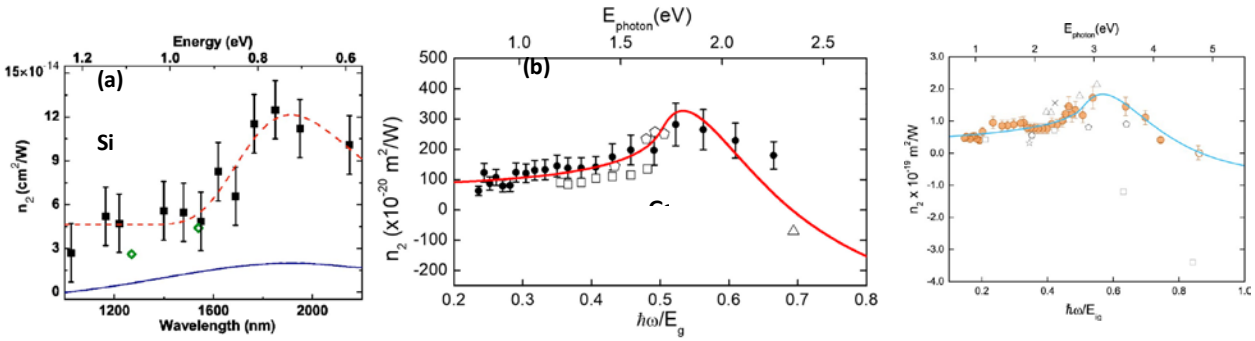

Figure 28.12 n_2 dispersion in (a) Si, (b) GaN, and (c) diamond

A table of nonlinear indices is given in Table 28.1

Material	n_0	$\chi^{(3)}$ (m^2/V^2)	n_2 (cm^2/W)	Comments and References
Crystals				
Al_2O_3	1.8	3.1×10^{-22}	2.9×10^{-16}	1
CdS	2.34	9.8×10^{-20}	5.1×10^{-14}	1,1.06 μm
Diamond	2.42	2.5×10^{-21}	1.3×10^{-15}	1
GaAs	3.47	1.4×10^{-18}	3.3×10^{-13}	1,1.06 μm
Ge	4.0	5.6×10^{-19}	9.9×10^{-14}	2, THG $\lvert\chi^{(3)}\rvert$
LiF	1.4	6.2×10^{-23}	9.0×10^{-17}	1
Si	3.4	2.8×10^{-18}	2.7×10^{-14}	2, THG $\lvert\chi^{(3)}\rvert$
TiO_2	2.48	2.1×10^{-20}	9.4×10^{-15}	1
ZnSe	2.7	6.2×10^{-20}	3.0×10^{-14}	1,1.06 μm
Glasses				
Fused silica	1.47	2.5×10^{-22}	3.2×10^{-16}	1
As_2S_3 glass	2.4	4.1×10^{-19}	2.0×10^{-13}	3
BK-7	1.52	2.8×10^{-22}	3.4×10^{-16}	1
BSC	1.51	5.0×10^{-22}	6.4×10^{-16}	1
Pb Bi gallate	2.3	2.2×10^{-20}	1.3×10^{-14}	4
SF-55	1.73	2.1×10^{-21}	2.0×10^{-15}	1
SF-59	1.953	4.3×10^{-21}	3.3×10^{-15}	1
Nanoparticles				
CdSSe in glass	1.5	1.4×10^{-20}	1.8×10^{-14}	3, nonres.
CS 3-68 glass	1.5	1.8×10^{-16}	2.3×10^{-10}	3, res.
Gold in glass	1.5	2.1×10^{-16}	2.6×10^{-10}	3, res.
Polymers				
Polydiacetylenes				
PTS		8.4×10^{-18}	3.0×10^{-12}	5, nonres.
PTS		-5.6×10^{-16}	-2.0×10^{-10}	6, res.
9BCMU			2.7×10^{-18}	7, $\lvert n_2\rvert$, res.
4BCMU	1.56	-1.3×10^{-19}	-1.5×10^{-13}	8, nonres, $\beta =$ 0.01 cm/MW
Liquids				
Acetone	1.36	1.5×10^{-21}	2.4×10^{-15}	9
Benzene	1.5	9.5×10^{-22}	1.2×10^{-15}	9
Carbon disulfide	1.63	3.1×10^{-20}	3.2×10^{-14}	9, $\tau = 2$ psec
CCl_4	1.45	1.1×10^{-21}	1.5×10^{-15}	9
Diiodomethane	1.69	1.5×10^{-20}	1.5×10^{-14}	9
Ethanol	1.36	5.0×10^{-22}	7.7×10^{-16}	9
Methanol	1.33	4.3×10^{-22}	6.9×10^{-16}	9
Nitrobenzene	1.56	5.7×10^{-20}	6.7×10^{-14}	9
Water	1.33	2.5×10^{-22}	4.1×10^{-16}	9
Other materials				
Air	1.0003	1.7×10^{-25}	5.0×10^{-19}	10
Ag		2.8×10^{-19}		2, THG $\lvert\chi^{(3)}\rvert$
Au		7.6×10^{-19}		2, THG $\lvert\chi^{(3)}\rvert$

Table 28.1 Nonlinear index of refraction and third order susceptibility of select materials

Four wave mixing (FWM)

Let us look at the response of a nonlinear medium to the two-tone field $E_{1,2} = A_{1,2}e^{j(\mathbf{k}_{1,2}\cdot\mathbf{r}-\omega_{1,2}z)}$ as described by (28.67)

$$\Delta\chi(\omega_{1,2}) \approx \frac{\chi(\omega_{1,2})\alpha n\tau}{N_a\hbar\omega\eta_0}\left[|A_1|^2 + |A_2|^2 + \frac{1}{1-j\Delta\omega\tau}A_1A_2^*e^{j(\Delta kz-\Delta\omega t)} + \frac{1}{1+j\Delta\omega\tau}A_1^*A_2e^{-j(\Delta kz-\Delta\omega t)}\right] \tag{28.73}$$

where $\Delta\mathbf{k} = \mathbf{k}_1 - \mathbf{k}_2$. The last two terms present a grating of with period $2\pi / \Delta k$ of both refractive index and absorption. This grating oscillates at frequency $\Delta\omega = \omega_1 - \omega_2$

When multiplied by $A_2 e^{\mathbf{j}(\mathbf{k}_2 \cdot \mathbf{r} - \omega_2 t)}$, the third term engenders nonlinear polarization at frequency $\Delta\omega + \omega_2 = \omega_1$, but the last term generates nonlinear polarization at new frequency $-\Delta\omega + \omega_2 = 2\omega_2 - \omega_1$,Similarly, scattering $A_1 e^{j(\mathbf{k}_1 \cdot \mathbf{r} - \omega_1 t)}$ off the third term generates polarization at frequency $\Delta\omega + \omega_1 = 2\omega_1 - \omega_2$. Those are FWM terms which cause new frequencies to appear. Similar phenomenon can of course be observed in the tPA –related nonlinearity, so in general we can generate polarization at the third frequency as

$$P_{TPA}^{(3)}(\omega_3) = \chi^{(3)}(\omega_3; \omega_2, \omega_2, -\omega_1) A_2^2 A_1^* e^{j((2\mathbf{k}_2 - \mathbf{k}_1)\cdot \mathbf{r} - \omega_3 t}$$
$$P_{TPA}^{(3)}(\omega_1) = \chi^{(3)}(\omega_3; \omega_2, \omega_2, -\omega_3) A_2^2 A_3^* e^{j((2\mathbf{k}_2 - \mathbf{k}_3)\cdot \mathbf{r} - \omega_1 t} \quad (28.74)$$

If E_2 is strong it can be considered as a pump, and the other two waves as signal and idler. As shown in Fig.28.13 a FWM is a third order parametric process in which two pump photons get transformed into signal and idler. The difference from the second order parametric amplification and generation is that all four photons have comparable energies (frequencies)

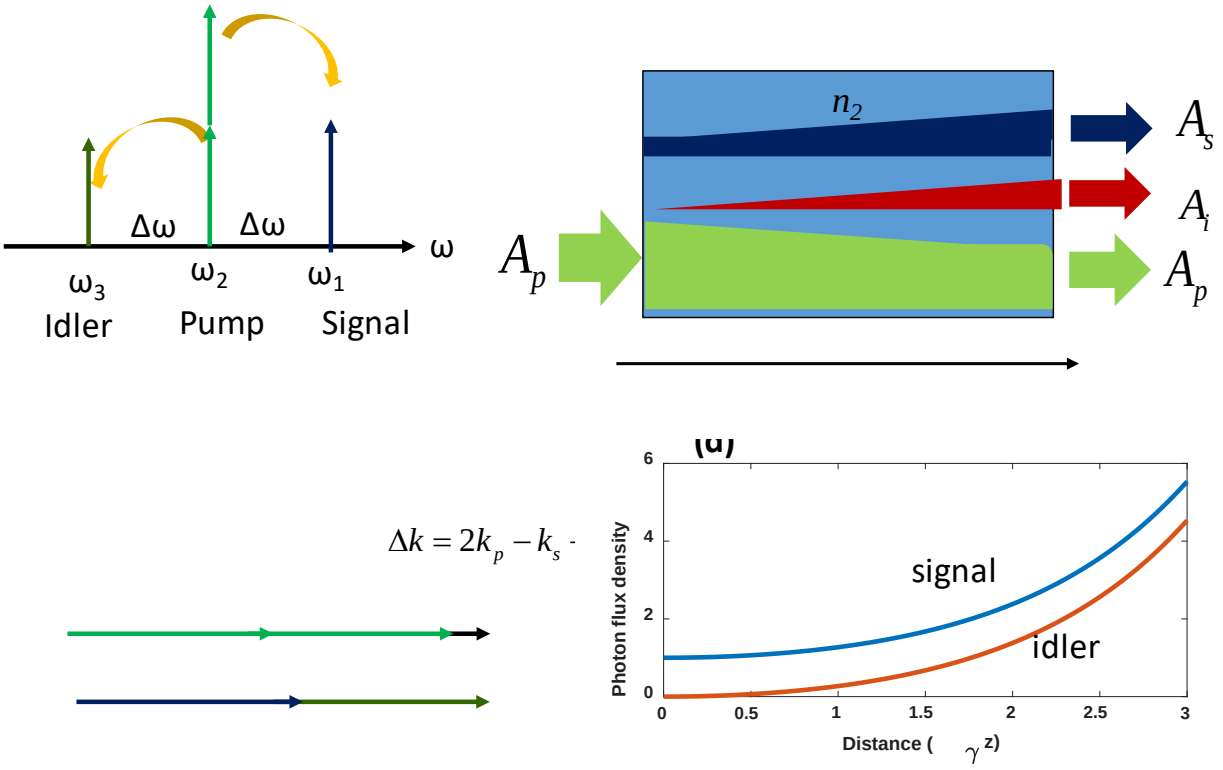

Figure 28.13 (a) New frequency generation via FWM (b) Waves propagation in FWM (c) Phase matching in the FWM (d) Evolution of signal and idler with undepleted pump

In Fig. 28.13 b we show collinear propagation of three waves. Since according to (28.55) $\mathrm{n}_2 \approx \chi^{(3)}\eta_0 / 4n^2$ and also according to (28.40) $S_p = 2n_{1,2} \mid A_p \mid^2 / \eta_0$,

$$\chi^{(3)} A_p^2 = 4n^2 \mathrm{n}_2 A_p^2 / \eta_0 = 2\mathrm{n}_2 n S_p \tag{28.75}$$

And nonlinear polarizations at signal and idler frequencies are from (28.74)

$$\begin{aligned} P^{(3)}(\omega_i, z) &= \varepsilon_0 \chi^{(3)} A_p^2 A_s^* e^{-j\omega_i t} e^{j(2k_p - k_s)z} = 2\varepsilon_0 \mathrm{n}_2 n S_p e^{-j\omega_i t} e^{j(2k_p - k_s)z} \\ P^{(3)}(\omega_s, z) &= \varepsilon_0 \chi^{(3)} A_p^2 A_i^* e^{-j\omega_i t} e^{j(2k_p - k_i)z} = 2\varepsilon_0 \mathrm{n}_2 n S_p A_i^* e^{-j\omega_i t} e^{j(2k_p - k_i)z} \end{aligned} \tag{28.76}$$

Upon substitution into the wave equation for slow variable amplitudes and assuming no pump depletion we obtain

$$\begin{aligned} \frac{dA_s}{dz} &= j\frac{\omega_s}{c} \mathrm{n}_2 S_p A_i^* e^{j\Delta k z} \\ \frac{dA_i}{dz} &= j\frac{\omega_i}{c} \mathrm{n}_2 S_p A_s^* e^{j\Delta k z} \end{aligned} \tag{28.77}$$

Where wavevector (momentum) mismatch is $\Delta k = 2k_p - k_s - k_i$ as shown in Fig.28.13.c. Let us find out the mismatch by expanding the wavevector into Taylor series

$$\begin{aligned} &\Delta k = 2k(\omega_p) - k(\omega_p + \Delta\omega) - k(\omega_p - \Delta\omega) = \\ &= 2k(\omega_p) - \left[k(\omega_p) + \frac{dk}{d\omega}\Delta\omega + \frac{1}{2}\frac{d^2k}{d\omega^2}\Delta\omega^2 \right] - \left[k(\omega_p) - \frac{dk}{d\omega}\Delta\omega + \frac{1}{2}\frac{d^2k}{d\omega^2}\Delta\omega^2 \right] = \beta_2 \Delta\omega^2 \end{aligned} \tag{28.78}$$

where, as always , $\beta_2 = \frac{d^2k}{d\omega^2}$ is the group velocity dispersion (GVD). The coherence length for FWM is therefore

$$L_c = \frac{\pi}{\beta_2 \Delta\omega^2} = \frac{1}{4\pi\beta_2 \Delta\nu^2} \tag{28.79}$$

Let is look at the examples. Assumed fused silica with $\beta_2 = 450\, fs^2 / cm$ and signal-pump difference $\Delta\nu = 1THz$ $(8nm)$. We obtain

$$L_c = \frac{1}{4\pi \cdot 450 \cdot 10^{-6}\, ps^2 / cm \cdot 1THz^2} \sim 180cm \tag{28.80}$$

Coherence length is much longer for FWM than for the second order parametric process, because all the frequencies are close to each other. If we consider optical fiber near its lowest dispersion wavelength of 1550nm, $\beta_2 = 10\, ps^2 / km$ and if we assume that we are talking about channels in fiber communication

link, the inter channel separation is $\Delta\nu = 100GHz\ (1nm)$ we obtain coherence length of $L_c = 800m$, almost a km long!

Now we can write coupled wave equations in case of perfect phase matching

$$\frac{dA_s}{dz} = j\frac{\omega_s}{c}\mathrm{n}_2 S_p A_i^* = j\frac{\gamma}{2}A_i^*$$
$$\frac{dA_i^*}{dz} = -j\frac{\omega_i}{nc}\mathrm{n}_2 S_p A_s = -j\frac{\gamma}{2}A_s \qquad (28.81)$$

where the parametric gain is

$$\gamma = \frac{2\omega}{c}\mathrm{n}_2 S_p = \frac{4\pi}{\lambda}\mathrm{n}_2 S_p \qquad (28.82)$$

Actually these coupled wave equations look exactly like the ones for the second order parametric amplification (27.130) and the solution (assuming zero input for idler) is

$$A_s(z) = A_s(0)\cosh\frac{\gamma}{2}z$$
$$A_i(z) = A_s(0)\sinh\frac{\gamma}{2}z \qquad (28.83)$$

or

$$S_s(z) = S_s(0)\cosh^2\frac{\gamma}{2}z$$
$$S_i(z) = S_s(0)\sinh^2\frac{\gamma}{2}z \qquad (28.84)$$

as shown in Fig.28.13 d .

Wavelength conversion

Consider now fused silica optical fiber with $\mathrm{n}_2 = 3\times10^{-16}cm^2/W$, let us say pump power I s1W and the fiber cross-section is $100\mu m^2$ hence $S_p = 10^6 W/cm^2$ and $\gamma \sim 0.005m^{-1}$ is rather small, but since coherence length is 800m $\gamma L = 4$ and therefore total gain is $G = e^{\gamma L} \sim 50$ which is quite respectable.

One can use FWM for wavelength conversion in which the signal is modulated light carrying information and this information is being transferred to the idler. This can be performed in a special dispersion-compensated fiber with low GVD of 10km length as shown in Fig. 28.14.a, as well as in Si waveguide of only 1.5cmm length (but with a very strong amplified pump) as shown in Fig.28.14.b

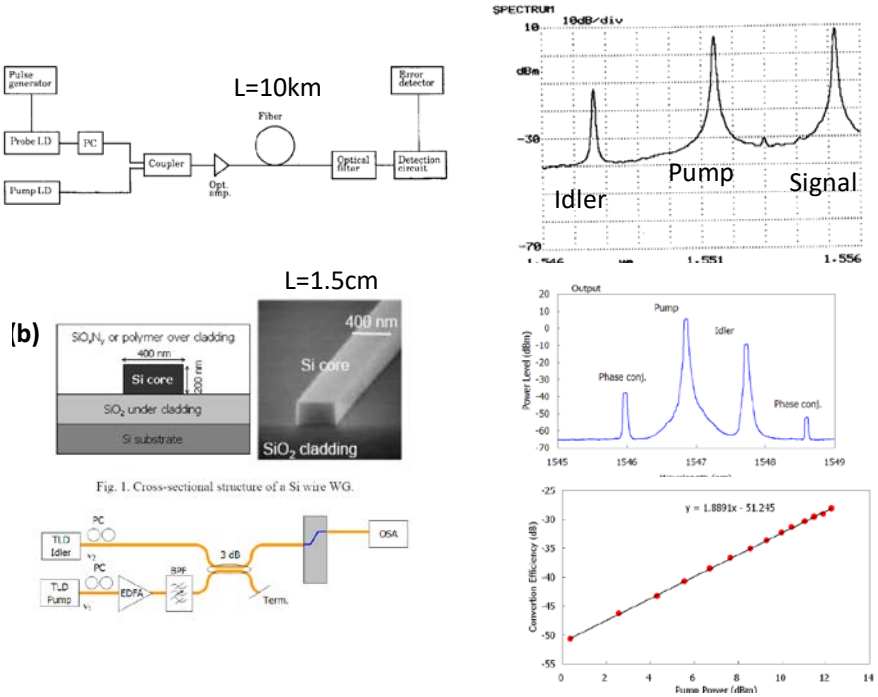

Figure 28.14 Wavelength conversion via FWM (a) in optical fiber (b) in Si waveguide

One can also perform wavelength conversion vis cross-phase modulation (XPM) in which the light in one channel gets modulated by the intensity of light in another channel as shown in Fig. 28.15

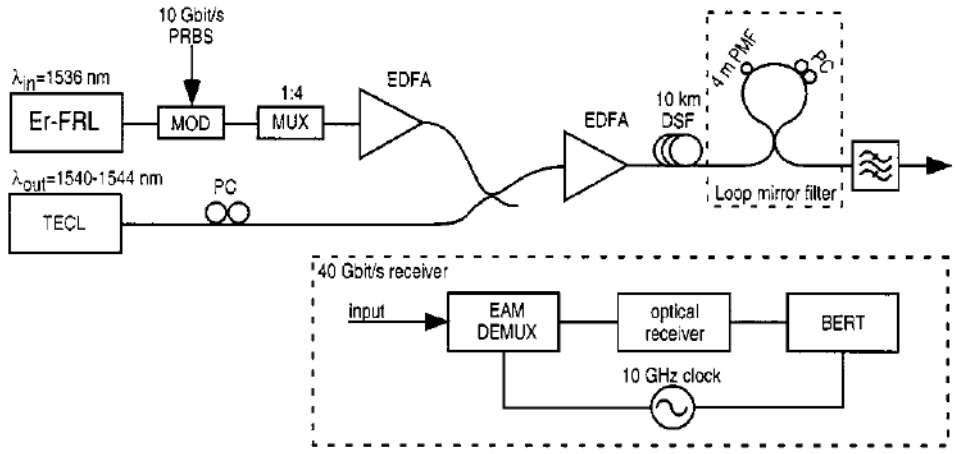

Figure 28.15. Wavelength conversion via XPM

Phase conjugation with degenerate FWM

Consider configuration of Fig.28.16a in which all waves have the same frequency ω. We have two counter propagating pumps

$$E_1 = A_1 e^{j(\mathbf{k}_1\cdot\mathbf{r}-\omega t)} + A_1^* e^{-j(\mathbf{k}_1\cdot\mathbf{r}-\omega t)}$$
$$E_2 = A_2 e^{j(\mathbf{k}_2\cdot\mathbf{r}-\omega t)} + A_2^* e^{-j(\mathbf{k}_2\cdot\mathbf{r}-\omega t)} \quad (28.85)$$

Interacting with a signal wave incident onto nonlinear medium

$$E_3 = A_3 e^{j(k_3 z-\omega t)} + A_3^* e^{-j(k_3 z-\omega t)} \quad (28.86)$$

Nonlinear polarization

$$P^{(3)}(\omega,\mathbf{r}) = \varepsilon_0 \chi^{(3)}(E_1+E_2+E_3)^3 \quad (28.87)$$

will include the "phase-conjugated" term

$$P_{PC}^{(3)}(\omega,\mathbf{r}) = 6\varepsilon_0\chi^{(3)} A_1 e^{j(\mathbf{k}_1\cdot\mathbf{r}-\omega t)} A_2 e^{j(\mathbf{k}_2\cdot\mathbf{r}-\omega t)} A_3^* e^{-j(\mathbf{k}_3\cdot\mathbf{r}-\omega t)} = 6\varepsilon_0\chi^{(3)} A_1 A_2 A_3^* e^{j(\mathbf{k}_1+\mathbf{k}_2-\mathbf{k}_3)\cdot\mathbf{r}-j\omega t} \quad (28.88)$$

Since $\mathbf{k}_1+\mathbf{k}_2=0$, and assuming undepleted equal power pumps so that

$$A_1 A_2 = S_p \eta_0 / 2n \quad (28.89)$$

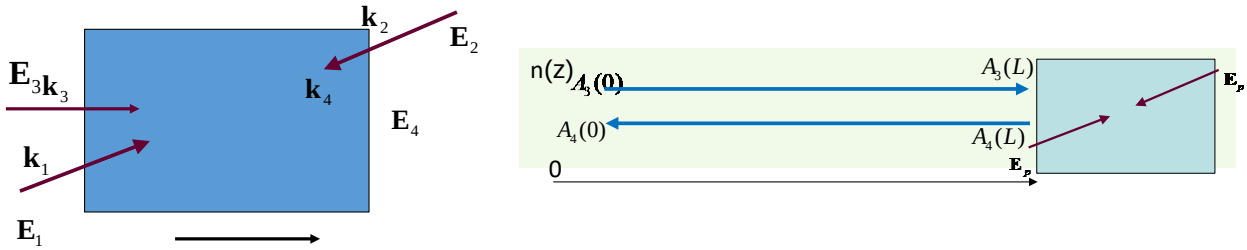

Figure 28.16 (a) waves involved in optical phase conjugation (b) Phase front correction with phase conjugation.

The nonlinear polarization

$$P_{PC}^{(3)}(\omega,r) = 2\varepsilon_0 \mathrm{n}_2 n S_p A_3^* e^{-j\mathbf{k}_3\cdot\mathbf{r}-j\omega t} = 2\varepsilon_0 \mathrm{n}_2 n S_p A_3^* e^{-jk_3 z-j\omega t} \quad (28.90)$$

engenders a new wave, propagating in the reverse direction –z ($\mathbf{k}_4 = -\mathbf{k}_3$)

$$E_4 = A_4 e^{-j(k_3 z+\omega t)} + A_4^* e^{j(k_3 z+\omega t)} \quad (28.91)$$

The propagation equation for it is

$$\frac{dA_4}{dz} = -j\frac{\omega}{c}\mathrm{n}_2 S_p A_3^* \quad (28.92)$$

and obviously wave 4 couples back into wave 3,

$$\frac{dA_3}{dz} = j\frac{\omega}{n}\mathrm{n}_2 S_p A_4^* \quad (28.93)$$

We finally obtain the coupled equations

$$\frac{dA_4}{dz} = -j\kappa A_3^*$$
$$\frac{dA_3}{dz} = j\kappa A_4^* \tag{28.94}$$

Where coupling coefficient is

$$\frac{\omega}{c} \mathrm{n}_2 S_p \tag{28.95}$$

and it can be positive or negative. Re-write (28.94) as

$$\frac{dA_4}{dz} = -j\kappa A_3^*$$
$$\frac{dA_3^*}{dz} = -j\kappa A_4 \tag{28.96}$$

and introduce $A_4 = jA_4^{'}$ so we have

$$\frac{dA_4^{'}}{dz} = -\kappa A_3^*$$
$$\frac{dA_3^*}{dz} = \kappa A_4^{'} \tag{28.97}$$

The prime can be dropped as 90 degrees' constant phase shift is not important. Solution I similar to the solution of Eq. (27.123) but with different boundary conditions

$$A_4(z) = B\cos(|\kappa| z) + C\sin(|\kappa| z)$$
$$A_3^*(z) = \frac{|\kappa|}{\kappa} B\sin(|\kappa| z) - \frac{|\kappa|}{\kappa} C\cos(|\kappa| z) \tag{28.98}$$

Boundary conditions are $A_3^*(0) = A_{3,0}^*$ $A_4(L) = 0$. Substituting them into (28.98) we obtain

$$B\cos(|\kappa| L) + C\sin(|\kappa| L) = 0$$
$$A_{30}^* = -\frac{|\kappa|}{\kappa} C \tag{28.99}$$

Hence

$$C = -\frac{\kappa}{|\kappa|} A_{3,0}^*$$
$$B = \frac{\kappa}{|\kappa|} \tan(|\kappa| L) A_{3,0}^* \tag{28.100}$$

We aer interested in

$$A_4(0) = B = \text{sign}(\kappa)\tan(|\kappa| L) A_{3,0}^*$$

$$A_3^*(L) = \left[\tan\left(|\kappa| L\right)\sin(|\kappa| L) + \cos(|\kappa| L)\right] A_{3,0}^* = \frac{A_{3,0}^*}{\cos(|\kappa| L)} \tag{28.101}$$

Both signal and phase conjugate signal get amplified and if $|\kappa| L = \pi / 2$ self-starting oscillation may occur ..

But let us now look at what the phase conjugation is good for. Consider the situation depicted in Fig.28.16b in which the incoming signal passes through the medium with refractive index n(z). The signal at z=0 is $A_3(0)$ and at point z=L where it inters PC crystal the signal is $A_3(L) = A_3(0)e^{j\Phi}e^{-j\omega t} + c.c.$ where the phase $\Phi = \frac{\omega}{c}\int_0^L n(z)dz$. Now, according to (28.101) the conjugate signal at z=L is $A_4(L) = A_3(0)e^{-j\Phi}e^{-j\omega t} + c.c.$- as the conjugate signal propagates back to 0 it becomes

$$A_4(L) = A_3(0)e^{j\Phi} = A_3(0)e^{-j\omega t} + c.c. \tag{28.102}$$

As one can see all the distortion caused by index variations have disappeared. Therefore, PC can be used to compensate the distortions caused by atmosphere as shown in Fig.28.17. In Fig.2716 athe difference between conventional mirror and PC mirror is shown. Normal mirror leaves the diverging wavefront diverging, but the PC mirror inverts phase and makes it converging.

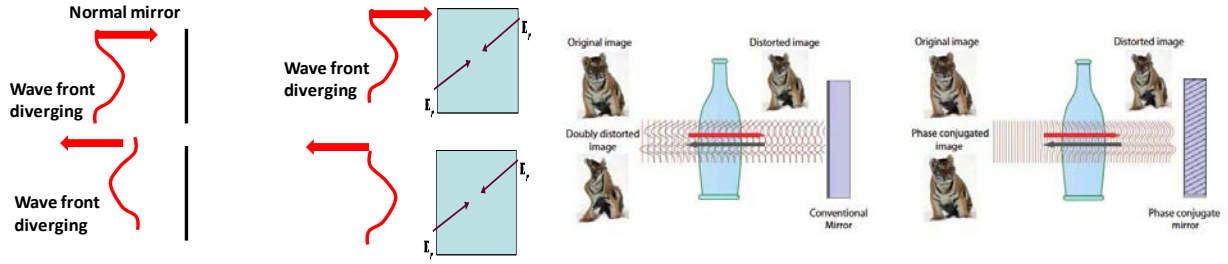

Figure 28.17 (a) Difference between conventional and PC mirrors (b) distortion correction using PC mirror

Self-focusing and self-trapping of light

To understand the effect of self-focusing consider a Gaussian beam with waist radius w_0 from Chapter 19, whose power density according to Eq 19.16 is

$$S = S_0 e^{-r^2/w_0^2} = \frac{P}{\pi w_0^2} e^{-r^2/w_0^2} \tag{28.103}$$

as shown in Fig.28.18.a Since the medium is nonlinear its refractive index acquires Gaussian profile which can be approximated as parabolic

$$n(r) = n_0 + \text{n}_2 S_0 e^{-r^2/w_0^2} \approx n_0 + \text{n}_2 S_0 (1 - r^2 / w_0^2) \tag{28.104}$$

with a radial gradient

$$\nabla n = -2n_2 S_0 r\hat{\mathbf{r}} / w_0^2 = -a^2 n_0 r\hat{\mathbf{r}};\quad a = \sqrt{2n_2 S_0 / n_0 w_0^2} \tag{28.105}$$

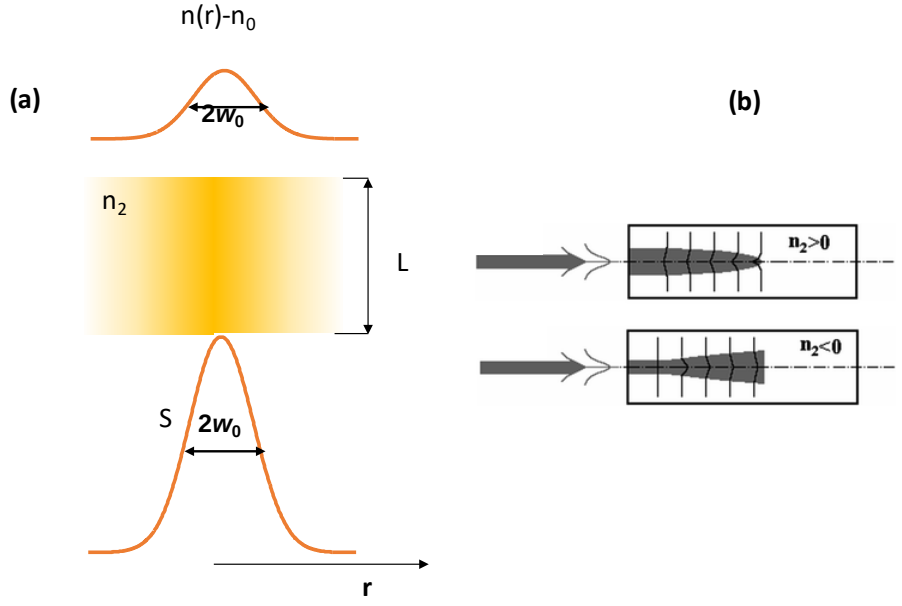

Figure 28.18 (a) Gaussian beam inducting the nonlinear lens (b) Self-focusing and de-focusing depending on sign of n_2

Now, according to Chapter 13 on graded index optics, we have an optically induced gradient index lens, which is positive (negative) and causes self-focusing (self de-focusing) depending on the sign of nonlinear index as shown in Fig.28.18b. To follow, according to Eq. (13.50), the equation of ray propagation is

$$\frac{d^2 r}{dz^2} = -a^2 r \tag{28.106}$$

having a solution

$$r(z) = r_0 \cos(az) \tag{28.107}$$

As one can see from Fig. 28.19a , assuming positive n_2, the light will converge in a tight spot at a distance of

$$z_{sf} = \frac{\pi}{2a} = \frac{\pi w_0}{2\sqrt{2n_2 S_0 / n_0}} = \frac{\pi^{3/2} w_0^2}{2^{3/2}} \sqrt{\frac{n_0}{n_2 P}} \tag{28.108}$$

called self-focusing length. The self-focusing angle can be estimated as

$$\theta_{sf} \approx \frac{w_0}{z_{sf}} = \frac{2}{\pi}\sqrt{2n_2 S_0 / n_0} \tag{28.109}$$

Interestingly enough, this angle depends only on power density and not on the actual beam radius.

The beam is also subjected to the divergence due to diffraction with divergence angle

$$\theta_{div} = 2\sqrt{2}\lambda / n_0 \pi w_0 \tag{28.110}$$

Effectively, one can find the combine convergence angle as

$$\theta = \sqrt{\theta_{sf}^2 - \theta_{div}^2} \approx \sqrt{\frac{8n_2 S_0}{\pi^2 n_0} - \frac{8\lambda^2}{\pi^2 n_0^2 w_0^2}} = \frac{2\sqrt{2}\lambda}{\pi n_0 w_0}\sqrt{\frac{n_2 S_0 n_0 w_0^2}{\lambda^2} - 1} = \theta_{div}\sqrt{\frac{n_2 P n_0}{\pi\lambda^2} - 1} = \theta_{div}\sqrt{\frac{P}{P_{cr}} - 1} \tag{28.111}$$

Where the critical power is

$$P_{cr} = \pi\lambda^2 / n_2 n_0 \sim 10^6 - 10^8 W \tag{28.112}$$

If the thickness of the material is less than self-focusing length, the light will get focused outside of the nonlinear medium, but if the medium is thick enough, the light will eventually get trapped into athin filament as shown in simulations of Fig.19.b

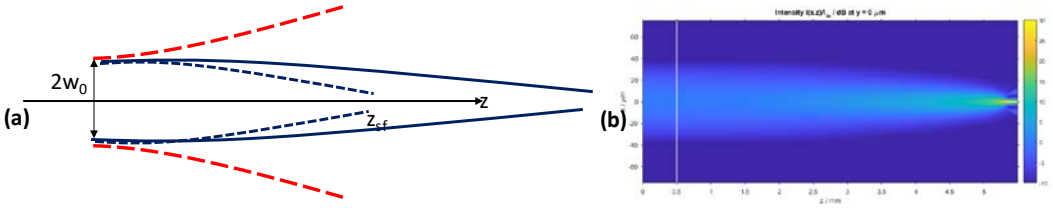

Figure 28.19 (a) Self focusing of light (b) Simulations of self-focusing and self-trapping

Self-focusing of light can be used to measure nonlinear index. As shown in Fig. 28.20 the sample is place between a lens and an aperture. The optically induced lens focal length depends on where the sample is placed, i.e. how tight is the beam on the sample, i.e. it changes as the sampled is moved along co-prdianet z (hence the name, z-scan) . Optically induced lens changes the beam radius at the aperture, hence the power which reaches the detector and one ends-up with the z-dependence shown in Fig.28.20 . From this curve the sign and the value of n_2 can be determined.

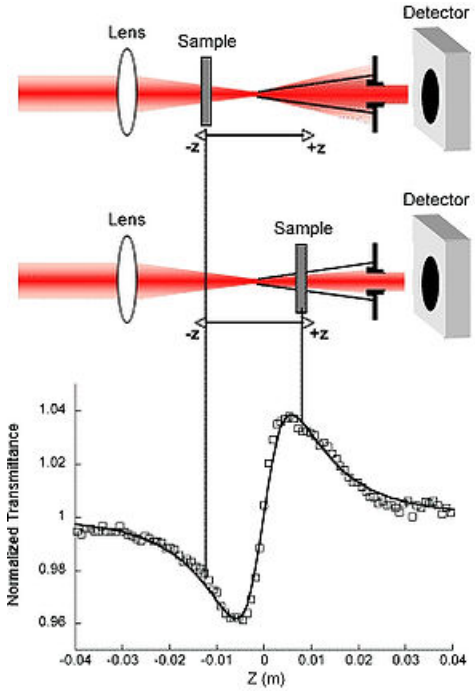

Figure 28.20 Z-scan measurement of nonlinear refractive index